Tribhuvan University Journal
Tribhuvan University • Kirtipur, Kathmandu, Nepal • ISSN 2091-0916 • Estd. 1964
Vol. 41, No. 1 | pp. 179–187
Year: 2026
Original Research Article
DOI:10.3126/tuj.v41i1.94597

Finite Element Modeling and Parametric Analysis of Concrete-Filled Steel Tube Stub Columns under Axial Compression

Arun Paudel[1], **Kabin Lamichhane**[1], **Arun Subedi**[1], **Ashim Paudel**[1], **Rabin Khadka**[1], **Sagar Baidhya**[1], **Avimanyu Lal Singh**[1], **Garima Gauli**[2,*]

[1]Pulchowk Campus, Institute of Engineering, Tribhuvan University
[2]Kathmandu Upatyaka Khanepani Limited
[*]*Correspondence*: garimagauli31@gmail.com

Article History

Received: 30 April, 2026 Revised: 28 June, 2026
Accepted: 29 June, 2026 Published: 30 June, 2026

Scan to access

How to Cite:

Paudel, A., Lamichhane, K., Subedi, A., Paudel, A., Khadka, R., Baidhya, S., Singh, A. L., & Gauli, G. (2026). Finite element modeling and parametric analysis of concrete-filled steel tube stub columns under axial compression. *Tribhuvan University Journal, 41*(1), 179–187. https://doi.org/10.3126/tuj.v41i1.94597

Keywords

Concrete-filled steel tubular columns, Confined concrete, Ductility, FE modelling, Slenderness ratio

ABSTRACT

Concrete-filled steel tube (CFST) columns are composite structural members that combine the compressive strength of concrete with the confinement and ductility provided by a steel tube. Owing to the passive confinement mechanism and nonlinear material interaction, accurate numerical modeling of CFST behavior especially with high-strength concrete and thin-walled steel tubes remains challenging. This study presents a refined three-dimensional finite element model to simulate the axial compressive behavior of CFST stub columns. The model is developed using the concrete damaged plasticity framework, incorporating strain hardening–softening behavior for confined concrete and modified material parameters to capture confinement effects more accurately. The proposed model was validated against experimental results from the literature and laboratory tests, showing close agreement in load–strain response, stiffness, ultimate load, ductility, and deformation pattern; in the laboratory comparison, the numerical and experimental responses matched closely up to about 130 kN. Following validation, parametric analyses were conducted to evaluate the influence of concrete grade, steel tube thickness, slenderness ratio, and binding bars on CFST axial compression performance. Increasing steel tube thickness from 1.5 mm to 5.5 mm significantly enhanced yield capacity, increasing it from approximately 1,550 kN to 2,600 kN for M20 concrete, 1,995 kN to 2,800 kN for M25 concrete, and 2,050 kN to 3,100 kN for M30 concrete. Concrete grade mainly improved initial stiffness and yield strength, while post-yield behavior was governed largely by steel confinement. For stub columns with L/D ratios from 1.81 to 10.91, the axial force–strain response remained nearly identical up to yield, indicating limited slenderness influence within the short-column range. Although binding bars increased initial stiffness, they reduced post-yield strength and ductility due to stress concentration effects. A comparative cost assessment also showed that a CFST column carrying 1,287 kN was about 16.8% cheaper than an equivalent RC column. The findings provide useful insight for the efficient modeling and practical design of CFST stub columns under axial compression.

Introduction

The demand for safer, taller, and more efficient structures has driven a growing interest in composite construction systems worldwide (Aznaw, 2025; Ali and Moon, 2018). Among these, concrete-filled steel tubular (CFST) columns have attracted extensive research and practical application because of their superior load-carrying capacity, ductility, energy absorption, and resistance to local and global buckling (Patel et al., 2018). The synergy between the confining steel tube and the infilled concrete enhances structural performance beyond what either material can achieve alone (Chen et al., 2023). As a result, CFST columns are now widely used in high-rise buildings, bridges, offshore platforms, and other critical infrastructure across seismic and non-seismic regions alike (Han, 2024; Han et al., 2014). In earthquake-prone countries, the advantages of CFST are particularly significant. The reduced structural mass, combined with high confinement efficiency, leads to better seismic performance compared to conventional reinforced concrete (RC) frames (Huang, 2015). Numerous experimental and numerical studies have confirmed the reliability of CFST under axial, flexural, and combined loading, establishing it as a mature and widely accepted structural solution (Han et al., 2014; Tao et al., 2013).

Nepal, however, continues to rely predominantly on RC moment-resisting frames for residential and public buildings. The 2015 Gorkha earthquake exposed the vulnerability of such systems: while many RC buildings remained standing, widespread damage and costly repairs highlighted their limited ductility and poor energy dissipation capacity. This event reinforced the need to explore alternative structural systems that can better balance strength, economy, ductility, and seismic resilience. Despite the global progress of CFST technology, its application and systematic study remain almost non-existent in Nepal, creating a clear need to evaluate the axial compression behavior of CFST columns using material grades, detailing practices, and construction conditions relevant to Nepal.

A review of international literature shows a strong focus on experimental testing, analytical modeling using finite element (FE) simulations of CFST columns (Sakino & Hayashi, 1991; Wang et al., 2009; Hassan et al., 2015). State-of-the-art FE approaches, particularly those employing the concrete damaged plasticity model, have demonstrated high accuracy in predicting confined concrete behavior and composite interaction (Tao et al., 2013). Parametric studies worldwide have also established the influence of steel tube thickness, concrete grade, and confinement measures on axial load capacity and ductility. Yet, these findings have not been contextualized to Nepal's construction practices, material availability, and seismic design requirements.

This study aims to evaluate the axial compression behavior of CFST stub columns for potential application in Nepalese construction. The specific objectives are to develop and validate a three-dimensional finite element model, compare the numerical response with experimental and literature-based results, and quantify the effects of steel tube thickness, concrete grade, slenderness ratio, and binding bar arrangement on load capacity, stiffness, and ductility. The scope of the study is limited to short CFST columns under concentric axial compression; however, the findings provide a useful basis for future seismic performance studies and practical CFST application in Nepal.

Materials and Methods

Numerical Modelling

Finite element Modeling

In any finite element based analysis, selection of the appropriate element type is instrumental to the success of the computational procedure. The Abaqus Standard module inset in ABAQUS 6.14.4 is used for modelling. The Abaqus Standard module consists of a comprehensive element library that provides different types of elements catering to different situations.

Material models

The cross sections of the CFST columns in this investigation is basically circular section. To achieve this goal, proper material constitutive models for steel tube and concrete are proposed. Then the proposed material constitutive models are verified against experimental data of Schneider (1998) and Huang et al. (2002). In the analysis, the Poisson's ratio and the elastic modulus of the steel tube are assumed to be 0.3 and 200 GPa. In this study, the Poisson's ratio of concrete was taken as 0.2.

Material modelling of steel

Different stress (σ)–strain (ε) models have been used for the steel material by different researchers, including elastic-perfectly plastic model, and elastic-plastic model with linear hardening or multi-linear hardening. At strains of general structural interest (Normally less than 5%), steel exhibits no significant strain hardening. For the elastic-plastic model with linear hardening, the strain hardening modulus (E_{p}) was taken as $0.005E_{\mathrm{S}}$, where E_{S} is the steel modulus of elasticity. A σ–ε model was proposed by Tao et al. for structural steel with a validity range of f_{y} from 200 MPa to 800 MPa. This model was used to simulate the steel material in circular CFST columns, which is expressed as follows:

$$\sigma(\varepsilon) = \begin{cases} E_{\mathrm{S}}\,\varepsilon, & \varepsilon \le \varepsilon_y, \\ f_y + E_p(\varepsilon - \varepsilon_y), & \varepsilon_y < \varepsilon \le \varepsilon_p, \\ f_u\left[1 - \left(\dfrac{\varepsilon - \varepsilon_p}{\varepsilon_u - \varepsilon_p}\right)^p\right], & \varepsilon > \varepsilon_p. \end{cases} \quad (1)$$

In which f_{u} is the ultimate strength; ε_y is the yield strain, $\varepsilon_y = f_y/E_{\mathrm{S}}$; ε_p is the strain at the onset of strain hardening; ε_u is the ultimate strain corresponding to the ultimate strength; p is the strain-hardening exponent, which can be determined by

$$p = \frac{\ln\left(\dfrac{f_u - f_y}{E_p(\varepsilon_u - \varepsilon_p)}\right)}{\ln\left(\dfrac{\varepsilon_u - \varepsilon_p}{\varepsilon_p - \varepsilon_y}\right)} \quad (2)$$

In which E_{p} is the initial modulus of elasticity at the onset of strain-hardening, and can be taken as 0.02Es. ε_p and ε_u are determined using Eqs. (3) and (4), respectively.

$$\varepsilon_p = \varepsilon_y + \frac{f_u - f_y}{E_p}, \tag{3}$$

$$\varepsilon_u = \varepsilon_p + \frac{f_u - f_y}{p\,E_p}. \tag{4}$$

Therefore, the elastic-perfectly plastic model is used to simulate the steel material in rectangular CFST columns.

Material modelling of concrete

For a CFST column under axial compression, the concrete core expands laterally and is confined by the steel tube. This confinement is passive in nature, and can increase the strength and ductility of concrete. This mechanism is well understood and is often referred to as "composite action" between the steel tube and concrete.

Concrete damaged plasticity model

The concrete damaged plasticity model available in ABAQUS was used. Since this paper only deals with columns under monotonic loading, damage variables were not defined. Therefore, concrete nonlinearity was modelled as plasticity only. In this model, key material parameters to be determined include the ratio of the second stress invariant on the tensile meridian to that on the compressive meridian (K_c), dilation angle (ψ), and strain hardening/softening rule. Other parameters include the modulus of elasticity (E_c), flow potential eccentricity (e), ratio of the compressive strength under biaxial loading to uniaxial compressive strength (f_{b0}/f_c'), viscosity parameter and tensile behavior of concrete. For the FE model presented by Han et al. (2014), constant values of 30°, 0.1, 1.16 and 2/3 were used for ψ, e, K_c and f_{b0}/f_c', respectively.

$$K_c = \frac{f_{b0}}{f_c'} \tag{5}$$

$$\psi = 30^\circ \quad \text{(typical value used for confined concrete models)} \tag{6}$$

Although CFST stub columns are not sensitive to tensile behavior of concrete when subjected to axial compression, tension stiffening needs to be defined in ABAQUS. In the current model, the uniaxial tensile response was assumed to be linear until the tensile strength of concrete was reached, which was taken as $0.1f_c'$. Beyond this failure stress, the tensile softening response was characterized by means of fracture energy (GF). The following equation was used to define GF for tensile concrete:

$$G_F = 0.073\, f_c'^{0.18}\, d_{\max}^{0.32} \quad \text{(fracture energy, empirical form)} \tag{7}$$

Where f_c' is in MPa, $d_{\max}$ is the maximum coarse aggregate size (in mm). If d_{max} had not been reported in a reference, it was taken as 20 mm.

Finding K_c

The ratio of the second stress invariant on the tensile meridian to that on the compressive meridian (K_c) is one of parameters for determining the yield surface of concrete plasticity model. According to Yu et al., the following equation can be deduced to calculate K_c:

$$K_c = \frac{5.5 f_{b0}}{3f_c' + 5f_{b0}}. \tag{8}$$

Equivalently, the adopted strength-dependent approximation is

$$K_c = \frac{5.5}{5 + 2\,(f_c')^{0.075}}. \tag{9}$$

From this equation, it can be found that K_c decreases slightly from 0.725 to 0.703 when f_c' increases from 30 MPa to 100 MPa.

Dilation Angle (ψ)

Dilation angle (ψ) is one of parameters required for ABAQUS to define the plastic flow potential. The allowed value of ψ ranges from 0° to 56° in ABAQUS. Different constant values of ψ have been used by different researchers in the past. Most researchers adopted a value of 20° or 30° for confined concrete.

The following equation is then proposed based on regression analysis to determine ψ for circular columns.

$$\psi = \begin{cases} 56.3(1 - \xi_c), & \xi_c \le 0.5, \\ 6.672 \exp\left(\dfrac{7.4}{4.64 + \xi_c}\right), & \xi_c > 0.5. \end{cases} \tag{10}$$

Where the confinement factor ξ_c is expressed as

$$\xi_c = \frac{A_s f_y}{A_c f_c'}. \tag{11}$$

In which A_s and A_c are the cross-sectional areas of the steel tube and concrete, respectively.

Mesh

When a CFST column is subjected to axial compression, the infilled concrete core behaves as a single solid block that undergoes compression without any rotation. ABAQUS 6.14.4 provides a set of Solid (continuum) elements specially designed for such cases. The most commonly used elements are 4-node linear tetrahedron (C3D4), 6-node linear triangular prism (C3D8) and 8-node linear brick elements (C3D8). Each of these elements possesses three translational degrees of freedom (DOFs) at each node. It is observed that for CFST members, C3D4 and C3D6 elements provide slow convergence and require very fine mesh which increases computational time and effort. C3D8 brick elements are found to be most suited from both the accuracy as well as time required viewpoints. It can be used for complex nonlinear analysis involving contact, plasticity and large deformations.

The hollow steel tube can be meshed by using either the shell elements or the solid brick elements. However, in addition to the translational DOFs, the shell elements also possess rotational DOFs. This may give rise to compatibility issues at the junction of concrete core and steel tube, since the concrete core elements come with only translational DOFs. Hence, trials were performed using C3D8 elements to mesh the steel tube also. A single layer of these elements through the element thickness is found to reproduce the deformed shape of the tube with good accuracy.

Interface Modelling

In order to obtain all the above mentioned advantages from the CFST columns, it is pertinent that steel tube and concrete core composite must behave as a single member and not merely as a combination of two different materials. This makes the simulation of composite action between concrete and steel tube the single most important factor guiding the behaviour of the composite member. The normal contact between the two materials is provided using friction, with the inner surface of the steel tube as the slave surface. The coefficient of friction between the two surfaces is chosen as 0.6. Hard Contact is provided between the two surfaces, which causes the pressure to be transmitted across the two surfaces only when there is actual contact among them, while causing the surfaces to separate under the influence of a tensile force.

Loading and Boundary Conditions

The steel tube and the concrete core are left completely unrestrained in all directions to allow any possible deformation in the column. The bottom rigid plate is fixed completely using the encastre boundary condition applied at its reference node, while the loading was applied by providing total displacement in small increments at the top surface. The value of the total displacement was generally kept slightly higher than the maximum value for the same in the corresponding experimental investigation.

Laboratory Test

To evaluate the behavior of CFST columns, laboratory tests were conducted on both plain concrete cylinders and CFST stub columns (Table 1). The experimental program was designed to establish the compressive strength of the mix and to study the axial performance of CFST specimens with varying slenderness ratios. M10-grade concrete was designed and used for casting specimens. Nine cylindrical concrete samples with a diameter of 100 mm and height of 200 mm were prepared. Compressive strength tests were carried out at 7, 14, and 21 days of curing, with the 21-day strength taken as the reference value for comparison. Similarly, all CFST stub columns were fabricated using circular hollow steel tubes filled with the prepared concrete. Six CFST specimens were prepared with the same diameter and thickness but different heights in order to investigate the effect of slenderness ratio (L/D) on axial load behavior. The nominal specimen heights were 250 mm, 300 mm, and 350 mm. The properties of the steel tube were as follows:

Table 1. Properties of steel tube used to prepare CFST stub column

Parameters	Unit	Value
External diameter (D)	mm	137.46
Wall thickness (t)	mm	4.48
Yield strength (fy)	N/mm^2	250
Elastic modulus (Es)	N/mm^2	200,000

All concrete cylinders and CFST specimens were tested under monotonic axial compression at 21 days of curing using a compression testing machine. Load–deformation data were recorded for each specimen and used for subsequent analysis.

Results and Discussion

Validation of Proposed FEM Model

The precision of the numerical model was judged by comparing the results from the model against the experimental results of authors like Schneider (1998), Sakino and Hayashi (1991) and Tomii et al. (1977). The parameters under evaluation were: a) peak compressive load capacity, b) load vs. displacement response at the moving end, c) deformed shape of the column, d) stiffness, and e) Ductility. From the figures, it is evident that a good reproduction of the load deformation pattern can be obtained from the model. The experimental and the numerically obtained deformed shapes are observed to be in good agreement as shown in Fig. 1. In the present model, C3D8 eight-node brick elements were used because they are suitable for nonlinear analysis involving contact, material plasticity, and large deformation. Other ABAQUS elements such as C3D8R reduced-integration brick elements, C3D20R quadratic brick elements, C3D10 tetrahedral elements, and S4R shell elements for the steel tube may also be used to capture nonlinear behavior, depending on the required accuracy, mesh quality, and computational cost.

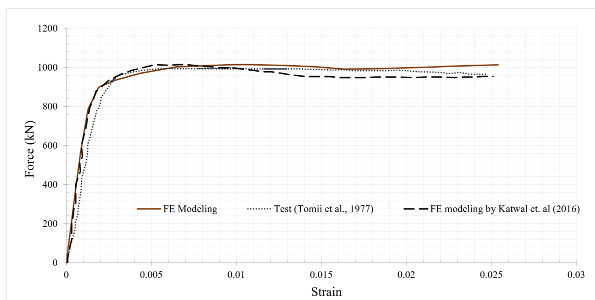

Fig. 1. Graphical comparison between the proposed modeling and test result for 3HN

Test Result

The proposed finite element model was used to calculate strain, displacement, and ultimate load of the tested CFST specimens. As shown in Fig. 2, the experimental and FE responses showed close agreement up to approximately 130 kN, indicating that the model captured the initial stiffness accurately. A slight deviation was observed beyond a strain of about 0.0025, mainly due to the nonlinear steel–concrete interaction and progressive confinement effect after yielding. Although the yield strain varied slightly, both responses showed similar ductile behavior.

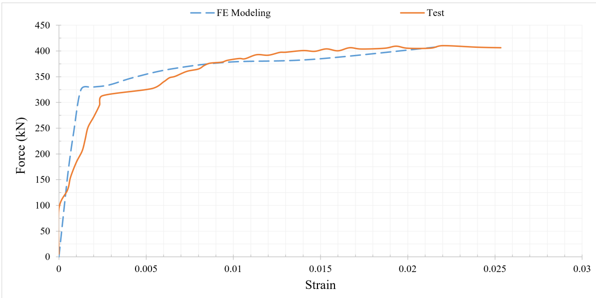

Fig. 2. Comparison between lab test and FEM results (Test 1), where the vertical axis represents force (kN) and the horizontal axis represents strain.

Combined Effect

The comparison of stress–strain responses (Fig. 3) shows that the concrete-filled steel tube (CFST) specimen possesses higher initial stiffness and yield strength than the simple arithmetic sum of the plain concrete and hollow steel tube tests. This improvement results from the composite interaction between steel and concrete: as the concrete core dilates under compression, the surrounding steel tube develops hoop tension that applies lateral confinement to the concrete. This confinement transforms the stress state of concrete from uniaxial to triaxial compression, thereby enhancing both its compressive strength and strain capacity. Simultaneously, the concrete core restrains inward buckling of the steel wall, allowing the tube to yield and harden in a more stable manner. Together, these mechanisms explain the steeper initial slope and higher yield point of the CFST curve compared to the non-composite case which is similar to the observation of Han et al. (2014) and Giakoumelis and Lam, (2004). This confirms that the improvement in CFST behavior is not simply the sum of the individual material strengths, but the result of confinement pressure developed at the steel–concrete interface and restraint against local inward buckling of the steel tube.

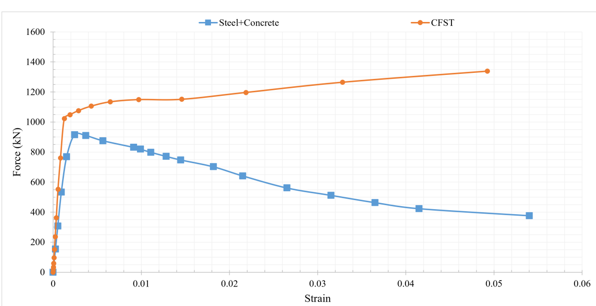

Fig. 3. Comparison of force–strain curves for CFST specimens and the arithmetic sum of individual concrete and hollow steel tube columns, where the vertical axis represents force (kN) and the horizontal axis represents strain.

Beyond yielding, the gap between the CFST and the "separate-sum" curve widens because confinement becomes more effective as the concrete expands laterally, while the steel experiences strain hardening. This interaction sustains load-carrying capacity and improves ductility, in contrast to the rapid post-peak decline of the unconfined concrete and thin-walled steel when tested separately. Prior studies (Zhao et al., 2022; Tao et al., 2011) confirm that CFSTs achieve superior ductility, ultimate strength, and energy absorption due to this synergy of confinement and buckling restraint, which cannot be reproduced by simply summing the strengths of their individual components.

Effect of slenderness ratio in short column

The ABAQUS simulations show that CFST stub columns with L/D ratios ranging from 1.81 to 10.91 exhibited nearly identical force–strain responses up to yield, with only marginal post-yield variation in load capacity (Fig. 4). This suggests that within the stub-column regime, axial strength and ductility are governed by composite interaction, specifically the active confinement of concrete by the steel tube and the restraint of the steel on local buckling, rather than by geometric slenderness variations. In contrast, standalone concrete specimens demonstrate a well-established sensitivity to L/D. As the aspect ratio increases, reported compressive strength tends to decrease due to reduced end-restraint and enhanced potential for buckling or fracture initiation.

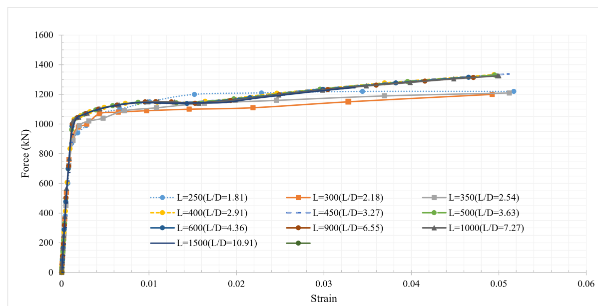

Fig. 4. Force–strain curves of CFST stub columns with varying L/D ratios (1.81, 2.18, 2.54, 2.91, 3.27, 3.63, 4.36, 6.55, 7.27, and 10.91), where the vertical axis represents force (kN) and the horizontal axis represents strain.

For instance, in rock (a brittle composite with similar failure mechanisms), sandstone shows a nonlinear decline in peak strength with increasing L/D, from about 194 MPa at L/D = 1.6 down to approximately 115 MPa at L/D = 2.0, reflecting a significant strength drop of over 40 MPa. The strength reduction slows as L/D grows further (Zhang et al., 2022). Even in standard concrete cores, the ASTM and BS codes prescribe correction factors: cylinders with L/D = 1.25 show strengths approximately 4 percent higher than those with L/D = 2.00 (Cook, 1989). These corrections underline the importance of L/D in isolated concrete testing. This L/D effect in concrete tests is the reason why standards such as ASTM and EN specify and normalize to a fixed L/D (commonly 2:1) for consistency. In CFST stub columns, however, the steel confinement and local stability mechanisms essentially neutralize L/D sensitivity across moderate slenderness values, maintaining consistent performance up to yielding.

Effect of Concrete Grade:

Fig. 5 clearly indicate that increasing the steel tube thickness in CFST stub columns substantially enhances both yield and ultimate load capacities across all tested concrete grades. For example, in M20-grade concrete, yield strength rose from approximately 1,550 kN for a 1.5 mm tube to about 2,600 kN for a 5.5 mm tube. Similarly, M25-grade specimens showed an increase from around 1,995 kN to 2,800 kN, and M30-grade specimens increased from roughly 2,050 kN to 3,100 kN. This trend suggests that thicker steel tubes offer stronger confinement and improved stability under axial compression, yielding nearly parallel strengthening trends across grade variations.

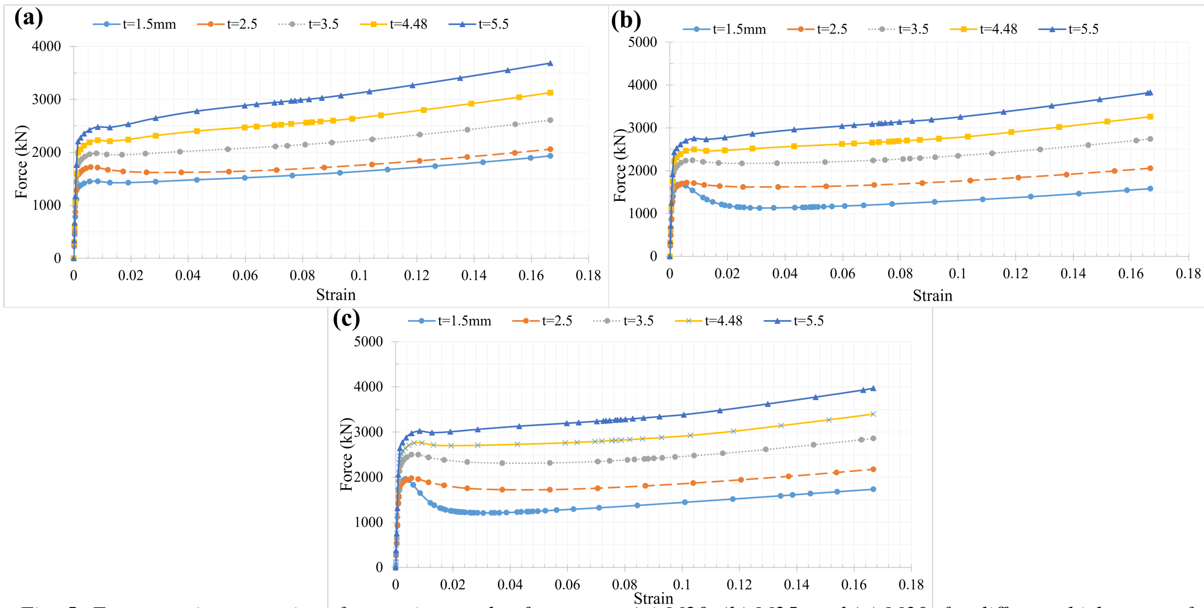

Fig. 5. Force–strain comparison for varying grade of concrete: (a) M20, (b) M25, and (c) M30; for different thicknesses of steel tube (t = 1.50 mm, t = 2.50 mm, t = 3.50 mm, t = 4.48 mm, and t = 5.50 mm), where the vertical axis represents force (kN) and the horizontal axis represents strain.

Such behavior is consistent with established findings in CFST research. Finite element studies and parametric investigations have shown that thicker steel tubes enhance concrete confinement, which in turn results in increased compressive strength. For instance, numerical analyses have demonstrated that increasing outer tube thickness leads to a linear increase in compressive strength of stub columns, owing directly to improved confinement performance (Shah and Ganesh, 2022). Moreover, parametric studies have shown that a lower diameter-to-thickness ratio (i.e., thicker tube) correlates with better axial capacity, while increasing D/t ratios (indicating thinner tubes) diminish ultimate load performance (Yadav & Chen, 2017). Therefore, the observed rise in yield and ultimate loads with increased tube thickness across varied concrete grades reflects the enhanced composite action and confinement efficiency produced by a more robust steel shell.

Effect of thickness of Steel Tube

The results displayed in Fig. 6 indicate that increasing the concrete grade enhances both yield and ultimate load capacities of CFST stub columns, regardless of steel tube thickness. For all tested tube thicknesses; 1.5 mm, 2.5 mm, and 4.48 mm, a near-parallel upward trend in yield strength is observed with increased concrete grade, and the increase in capacity is more pronounced in the yield region than at ultimate load. This trend suggests that higher-strength concrete contributes substantially to early stiffness and initial yield behavior, while post-yield enhancements are governed more by the steel tube confinement. The uniformity of this trend across varying steel thicknesses implies that confinement efficiency provided by the steel tube remains effective, enabling concrete grade improvements to translate directly into higher performance without significant interaction effects between thickness and grade.

These observations align closely with findings from existing parametric and finite element studies. Yadav and Chen (2017) demonstrated that the ultimate axial capacity of CFST columns increases with concrete grade, irrespective of changes in diameter-to-thickness ratios, reflecting the concrete's primary role in defining compressive strength. Similarly, Tiwary and Gupta (2021) highlight that increasing core concrete strength enhances stiffness and load-bearing capacity, although it may introduce brittleness in failure mode. Taken together, these studies underscore that improvements in concrete quality result in more substantial gains in early structural resistance, which remain consistent even as steel thickness varies. The results in Fig. 6 therefore validate these theoretical and numerical findings and affirm that concrete grade is a dominant factor in CFST column behavior.

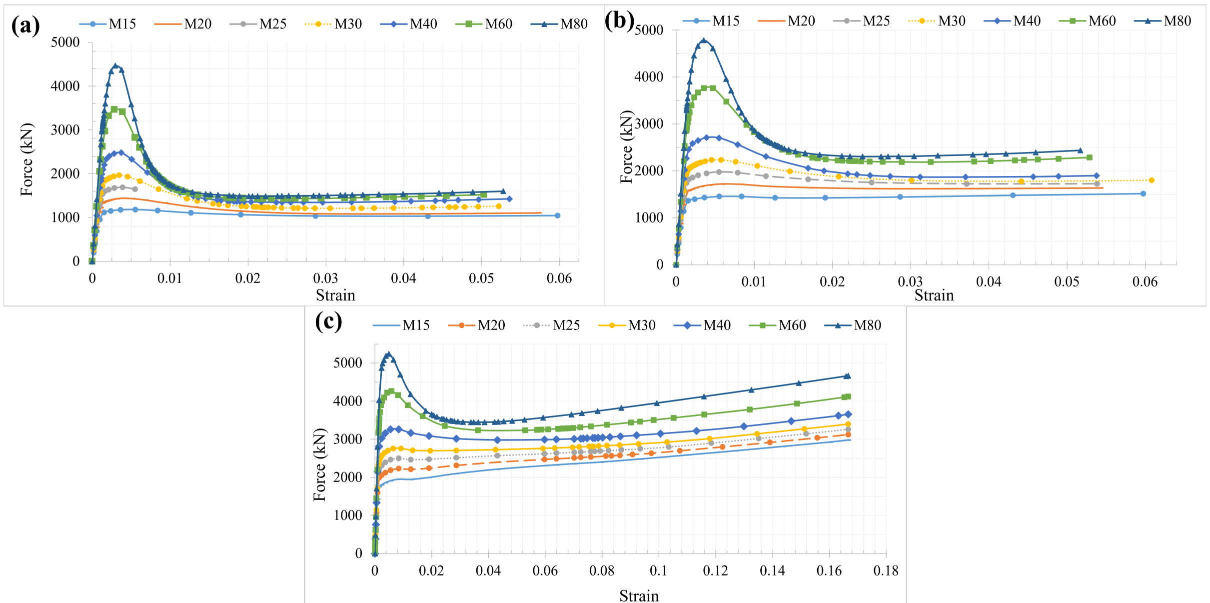

Fig. 6. Force–strain comparison for varying thickness of steel tube: (a) 1.50 mm, (b) 2.50 mm, and (c) 4.48 mm; for different grades of concrete (M15, M20, M25, M30, M40, M60, and M80), where the vertical axis represents force (kN) and the horizontal axis represents strain.

Cost Comparison of CFST column with RC column

To compare the cost of the column with these two material, a CFST column of 1.5m length, 137.46mm outer diameter and thickness 4.48mm filled with concrete of characteristic strength 14.17N/mm^2 was modelled in ABAQUS. Ultimate load carrying capacity of the model was determined to 1287KN. Then, a RCC column was designed to carry the same compressive load as a short column under axial compression only. The steel percentage of 2.5% was used to calculate the size of column and accordingly provided. The size of column required was found to be 364mm and hence a column of size 370*370mm was used for calculation. The cost of the RCC column may increase further by at least 10% due to formwork requirements, whereas the steel tube in a CFST column acts as permanent formwork. For the same axial load capacity of 1,287 kN, the CFST column was found to be approximately 16.8% cheaper than the equivalent RCC column.

Effect of binding bar On CFST

The influence of binding bars on joint performance was found to be significant. A similar strengthening concept was therefore extended to the column specimens. In this configuration, a pair of binding bars was provided at the mid-height of the column in a cruciform (cross) arrangement and welded at their ends to the steel tube. A corresponding numerical model was developed to capture the structural response of this configuration, and detailed analyses were carried out. For columns constructed using M20 grade concrete and Fe250 binding bars, the results are summarized in Fig. 7. The load–deformation responses indicate a noticeable modification in the structural behavior due to the inclusion of binding bars.

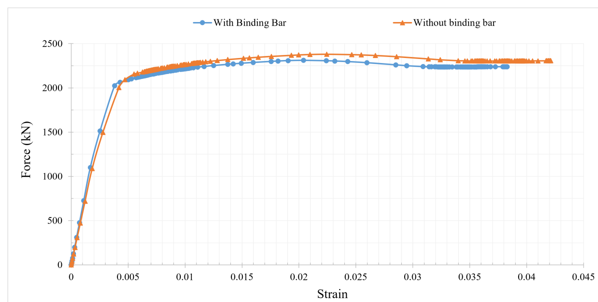

Fig. 7. Comparison of CFST column behavior with and without binding bars, where the vertical axis represents force (kN) and the horizontal axis represents strain.

Across all analyzed cases, the presence of binding bars led to an increase in the initial stiffness of the column system, as evidenced by the steeper slope of the initial portion of the load–displacement curves. This enhancement can be attributed to improved confinement and restraint provided by the binding bars, which delayed the onset of cracking and elastic deformation. However, beyond the yielding stage, a reduction in the ultimate load-carrying capacity was observed in comparison to the corresponding specimens without binding bars. The premature localization of stresses around the welded binding bars appears to have influenced post-yield behavior adversely, leading to earlier strength degradation.

Furthermore, the post-yield deformation capacity was reduced in the specimens with binding bars, indicating a decrease in overall ductility. Although the initial stiffness enhancement is beneficial from a serviceability perspective, the compromised ductility suggests that the use of binding bars may negatively affect the energy dissipation capacity of the column system under higher deformation demands. Therefore, although binding bars improved the initial stiffness response, their use in CFST columns should be carefully reconsidered because the welded regions may create local stress concentration and reduce post-yield deformation capacity.

Conclusion

This study investigated the axial compressive behavior of concrete-filled steel tube (CFST) stub columns using a validated finite element modeling approach. A three-dimensional numerical model was developed in ABAQUS and verified against established experimental results from the literature and selected laboratory observations, with the laboratory comparison showing close agreement between the numerical and experimental response up to approximately 130 kN. The validated model was then used to examine the effects of composite action, slenderness ratio, concrete grade, steel tube thickness, cost efficiency, and the introduction of binding bars on column performance. The results show that CFST columns perform significantly better than plain concrete or hollow steel tubes due to effective steel–concrete interaction, leading to higher stiffness, strength, and ductility. Steel tube thickness was found to be the most influential parameter, with yield capacity increasing from approximately 1,550 kN to 2,600 kN for M20 concrete, 1,995 kN to 2,800 kN for M25 concrete, and 2,050 kN to 3,100 kN for M30 concrete as tube thickness increased from 1.5 mm to 5.5 mm; higher concrete grades mainly enhanced initial stiffness and yield strength. Slenderness effects were minimal within the stub-column range considered, as specimens with L/D ratios from 1.81 to 10.91 showed nearly identical force–strain responses up to yielding. Although binding bars improved initial stiffness, they reduced post-yield strength and ductility, making them unsuitable for column applications without alternative detailing. In addition to structural advantages, the CFST column with 1.5 m length, 137.46 mm outer diameter, 4.48 mm tube thickness, and 1,287 kN ultimate load capacity was approximately 16.8% more economical than an equivalent reinforced concrete column, confirming its suitability as an efficient and cost-effective compression member in practical design.

Acknowledgment

Author would like to appreciate the team of Central Material Testing Laboratory and the Department of Civil Engineering.

Artificial Intelligence (AI) Use and Disclosure

In the preparation of this manuscript, AI tools were used for some sections, with minimal or no editing.

Similarity and Originality Confirmation

The manuscript is original, not under review elsewhere, and complies with TUJ publication ethics.

Conflict of Interest

The authors declare no conflict of interest.

Funding

State funding sources, grants, or declare no funding received.

Data Availability

Data available from the corresponding author on request.

Author declaration

I/We declare that all the information provided above is correct and the manuscript is fully compliant with the requirements for submission to the journal.

References

Ali, M. M., & Moon, K. S. (2018). Advances in structural systems for tall buildings: emerging developments for contemporary urban giants. *Buildings*, *8*(8), 104.

Aznaw, G. M. (2025). Advances in Composite Structures: A Systematic Review of Design, Performance, and Sustainability Trends. *Composite Materials*, *9*(1), 1-17.

Bridge, R. (1976). *Concrete filled steel tubular columns* (Research Report No. R283). School of Civil Engineering, University of Sydney, Sydney, Australia.

Chacón, R. (2015). Circular concrete-filled tubular columns: State of the art oriented to the vulnerability assessment. *The Open Civil Engineering Journal, 9*(Suppl. 1 M4), 249–259.

Chen, B., Liu, J., & Wei, J. (2023). *Concrete-filled steel tubular arch bridges*. Singapore: Springer.

Fouché, P., & Bruneau, M. (2010). Non-linear analysis of multi-hazard performance of concrete filled steel tubes bridge piers. In *Proceedings of the 8th International Conference on Short and Medium Span Bridges* (pp. Not available). Canadian Society for Civil Engineering (CSCE), West Montréal, QC, Canada.

Giakoumelis, G., & Lam, D. (2004). Axial capacity of circular concrete-filled tube columns. *Journal of Constructional Steel Research, 60*(7), 1049–1068. https://doi.org/10.1016/j.jcsr.2003.10.001 (iptek.its.ac.id)

Gupta, P. K., Sarda, S. M., & Kumar, M. S. (2007). Experimental and computational study of concrete filled steel tubular columns under axial loads. *Journal of Constructional Steel Research, 63*(2), 182–193.

Hajjar, J. F. (2000). Concrete-filled steel tube columns under earthquake loads. *Program on Structural Engineering and Materials, 2*(1), 72–81.

Han, L. H. (2001). Fire performance of concrete filled steel tubular beam columns. *Journal of Constructional Steel Research*.

Han, L. H., Li, W., & Bjorhovde, R. (2014). Developments and advanced applications of concrete-filled steel tubular (CFST) structures: Members. *Journal of constructional steel research*, *100*, 211-228.

Han, L. H. (2024). *Theory of concrete-filled steel tubular structures*. Springer.

Han, L.-H., Li, W., & Bjorhovde, R. (2014). Developments and advanced applications of concrete-filled steel tubular (CFST) structures: Members. *Journal of Constructional Steel Research, 100*, 211–228. https://doi.org/10.1016/j.jcsr.2014.04.016

Hu, H. T., Huang, C. S., & Wu, M. (2003). Nonlinear analysis of axially loaded concrete-filled tube columns with confinement effect. *Journal of Structural Engineering, 129*(10), 1322–1329.

Huang, Y. (2015). Seismic behavior of concrete filled steel tubular built-up columns.

Lu, Y., Zhou, F., & Liao, F. (2010). Fire performance of self-consolidating concrete filled double skin steel tubular columns: Experiments. *Fire Safety Journal, 45*(2), 106–115.

Lu, Y., Zhou, F., & Liao, F. (2011). FE modelling and fire resistance design of concrete filled double skin tubular columns. *Journal of Constructional Steel Research, 67*(11), 1733–1748.

Patel, V., Liang, Q. Q., & Hadi, M. (2018). *Concrete-filled stainless steel tubular columns*. CRC Press.

Qasim, O. A. (2018). A review paper on specimen size and shape effects on the concrete properties. *International Journal of Recent Advances in Science and Technology, 5*(3), 13–25.

Qi, M., Zhao, G., Xu, W., Cheng, X., Liu, C., Liu, Z., & Wu, X. (2022). Influence of height–diameter ratio on rock compressive failure characteristics and damage evolution law. *Energies, 15*(15), Article 5557. https://doi.org/10.3390/en15155557

Sakino, K., & Hayashi, H. (1991). Behavior of concrete filled steel tubular stub columns under concentric loading. In *Proceedings of the 3rd International Conference on Steel-Concrete Composite Structures* (pp. 25–30). Fukuoka, Japan.

Sakino, K., Nakahara, H., Morino, S., & Nishiyama, I. (2004). Behavior of centrally loaded concrete-filled steel-tube short columns. *Journal of Structural Engineering, 130*(2), 180–188.

Schneider, S. P. (1998). Axially loaded concrete filled steel tube. *Journal of Structural Engineering, 124*(10), 1125–1138.

Shah, S. M. I., & Ganesh, G. M. (2022). Impact of diameter to thickness (D/t) on axial capacity of circular CFST columns: Experimental, parametric and numerical analysis. *International Journal of Applied Science and Engineering, 19*(2), Article 2021486. https://doi.org/10.6703/IJASE.202206_19(2).005

Tao, Z., Wang, Z.-B., & Yu, Q. (2013). Stress-strain curves of structural and reinforcing steels after exposure to elevated temperatures. *Journal of Materials in Civil Engineering, 25*(9), 1306–1316.

Tomii, K., Yoshimura, M., & Morishita, Y. (1977). Experimental studies on concrete filled steel tubular stub columns under concentric loading. In *Proceedings of the International Colloquium on Stability of Structures Under Static and Dynamic Loads* (pp. 718–741). Washington, DC, USA.

Yadav, R., & Chen, B. (2017). Parametric study on the axial behaviour of concrete filled steel tube (CFST) columns. *American Journal of Applied Scientific Research, 3*(4), 21–25. https://doi.org/10.11648/j.ajasr.20170304.11

Tribhuvan University Journal (TUJ)
ISSN 2091-0916 • Est. 1964
Tribhuvan University, Kirtipur, Kathmandu, Nepal
nepjol.info/index.php/TUJ